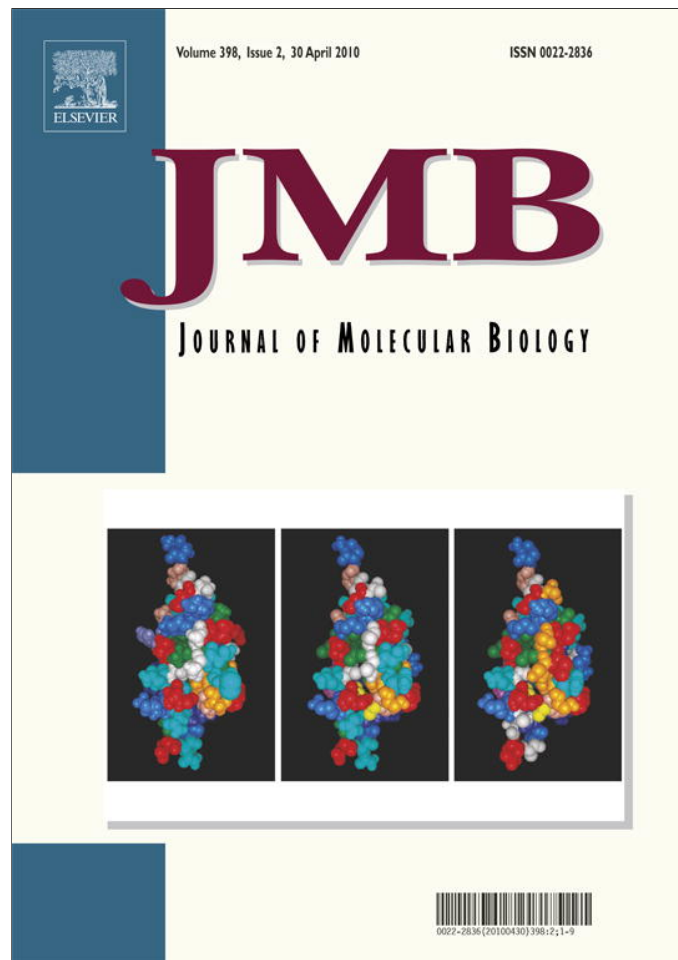


Provided for non-commercial research and education use.
Not for reproduction, distribution or commercial use.



This article appeared in a journal published by Elsevier. The attached copy is furnished to the author for internal non-commercial research and education use, including for instruction at the authors institution and sharing with colleagues.

Other uses, including reproduction and distribution, or selling or licensing copies, or posting to personal, institutional or third party websites are prohibited.

In most cases authors are permitted to post their version of the article (e.g. in Word or Tex form) to their personal website or institutional repository. Authors requiring further information regarding Elsevier's archiving and manuscript policies are encouraged to visit:

<http://www.elsevier.com/copyright>

JMB

Available online at www.sciencedirect.com

 ScienceDirect


Crystal Structure of Sulfide:Quinone Oxidoreductase from *Acidithiobacillus ferrooxidans*: Insights into Sulfidotrophic Respiration and Detoxification

Maia M. Cherney[†], Yanfei Zhang[†], Matthew Solomonson,
Joel H. Weiner and Michael N. G. James^{*}

Group in Protein Structure and Function, Department of Biochemistry, School of Molecular and Systems Medicine, Faculty of Medicine and Dentistry, University of Alberta, 4-31 Medical Sciences Building, Edmonton, Alberta, Canada T6G 2H7

Received 15 December 2009;
received in revised form
8 March 2010;
accepted 10 March 2010
Available online
19 March 2010

Sulfide:quinone oxidoreductase from the acidophilic and chemolithotrophic bacterium *Acidithiobacillus ferrooxidans* was expressed in *Escherichia coli* and crystallized, and its X-ray molecular structure was determined to 2.3 Å resolution for native unbound protein in space group $P4_22_12$. The decylubiquinone-bound structure and the Cys160Ala variant structure were subsequently determined to 2.3 Å and 2.05 Å resolutions, respectively, in space group $P6_222$. The enzymatic reaction catalyzed by sulfide:quinone oxidoreductase includes the oxidation of sulfide compounds H_2S , HS^- , and S^{2-} to soluble polysulfide chains or to elemental sulfur in the form of octasulfur rings; these oxidations are coupled to the reduction of ubiquinone or menaquinone. The enzyme comprises two tandem Rossmann fold domains and a flexible C-terminal domain encompassing two amphipathic helices that are thought to provide for membrane anchoring. The second amphipathic helix unwinds and changes its orientation in the hexagonal crystal form. The protein forms a dimer that could be inserted into the membrane to a depth of approximately 20 Å. It has an endogenous flavin adenine dinucleotide (FAD) cofactor that is noncovalently bound in the N-terminal domain. Several wide channels connect the FAD cofactor to the exterior of the protein molecule; some of the channels would provide access to the membrane. The ubiquinone molecule is bound in one of these channels; its benzoquinone ring is stacked between the aromatic rings of two conserved Phe residues, and it closely approaches the isoalloxazine moiety of the FAD cofactor. Two active-site cysteine residues situated on the *re* side of the FAD cofactor form a branched polysulfide bridge. Cys356 disulfide acts as a nucleophile that attacks the C4A atom of the FAD cofactor in electron transfer reaction. The third essential cysteine Cys128 is not modified in these structures; its role is likely confined to the release of the polysulfur product.

© 2010 Elsevier Ltd. All rights reserved.

Keywords: sulfide:quinone oxidoreductase; SQR–decylubiquinone complex; integral monotopic membrane protein; *Acidithiobacillus ferrooxidans*; X-ray crystallography

Edited by M. Guss

Introduction

Acidithiobacillus ferrooxidans is a Gram-negative, acidophilic, and chemolithotrophic bacterium that is usually found in acidic environments. It derives energy for growth mainly from oxidative respiration using reduced inorganic compounds such as Fe^{II} , H_2S , S^{2-} , S^0 , and Cu^I that are present in surrounding ores; ultimately, electrons are moved from these substrates to oxygen.^{1,2} Several redox proteins are involved in respiratory chains. One of the enzymes

^{*}Corresponding author. E-mail address:
michael.james@ualberta.ca.

[†] M.M.C. and Y.Z. contributed equally to this study.

Abbreviations used: FAD, flavin adenine dinucleotide; SQR, sulfide:quinone oxidoreductase; DSR, disulfide oxidoreductase; PDB, Protein Data Bank; FCC, flavocytochrome *c*:sulfide dehydrogenase; WT, wild type; DUQ, decylubiquinone; DDM, *n*-dodecyl β -D-maltoside.

responsible for the earlier stages in sulfide oxidation is sulfide:quinone oxidoreductase (SQR). SQR is an ancient flavoprotein of the disulfide oxidoreductase (DSR) family that is present in all domains of life (archaea, bacteria, and eukarya), thereby augmenting its original role in respiration. Initially, SQRs were found in sulfidotrophic bacteria. Later, SQR-like enzymes were also found in the mitochondria of some fungi, as well as in all animal species with known genome sequences.^{3,4} Based on a phylogenetic analysis of completed bacterial genomes, SQR genes were classified into at least two clades: type I and type II SQRs. Type I SQRs occur in a diverse range of bacteria, including *At. ferrooxidans*.^{5–7} They participate in respiration or anaerobic photosynthesis and are characterized by high substrate affinities and high reaction rates.^{6,7} Type II SQRs include those from other bacteria, as well as mitochondrial SQR-like enzymes. Type II SQRs are mostly involved in detoxification,³ heavy metal tolerance,^{8,9} and, presumably, signaling in higher eukaryotes by controlling the levels of H₂S in the brain.^{10–13} Additionally, ATP production in the mitochondria, with sulfides as electron donors, has been observed.^{14–16}

Similar to other members of the DSR family, SQRs are thought to be mainly dimeric (embedded in the cytoplasmic membrane on the periplasmic side),^{5,6} but some of them might be trimers.¹⁷ They are considered to be integral monotopic membrane proteins. The molecular mass of the monomeric enzyme is around 50 kDa. The enzyme usually harbors a covalently bound flavin adenine dinucleotide (FAD) cofactor in each monomer,^{17–19} but the FAD cofactor can also be bound noncovalently (as seen in the current structures; there are also reports about the loss of FAD in SQRs during purification).⁶ The enzymatic reaction catalyzed by SQR includes the oxidation of reduced sulfur compounds H₂S, HS⁻, and S²⁻ to soluble polysulfide chains⁶ or to elemental sulfur in the form of octasulfur rings.¹⁷ Electrons from the sulfides are transferred through FAD to the ubiquinone or menaquinone pool in the membrane.

The structures of SQRs from the hyperthermophilic bacterium *Aquifex aeolicus* [Protein Data Bank (PDB) codes 3hyx, 3hyv, and 3hyw] and from the hyperthermoacidophilic archaeon *Acidithiobacillus ambivalens* (PDB code 3h8l) have recently been reported.^{17,18} *At. ferrooxidans* SQR has 40% and 27% sequence identities with the abovementioned proteins, respectively. A related structure of the flavocytochrome *c*:sulfide dehydrogenase (FCC) from *Allochromatium vinosum* (PDB code 1fcd) that was reported about 15 years ago has a 24% sequence identity.¹⁹ The available structures shed light on the complex mechanism of electron transfer, but further investigation, including the structural data of SQRs from different species, is needed for a better understanding of catalytic events.

Here we present the three-dimensional structures of the *At. ferrooxidans* native unbound enzyme, the acceptor-bound enzyme, and the Cys160Ala variant SQR molecule.

Results

SQR enzymatic activity assays

Enzymatic activity assays have been carried out for the wild type (WT) and the Cys160Ala, Cys356Ala, and Cys128Ala variants in the absence of detergents. The WT protein showed the highest specific activity reported to date: 400–500 U/mg protein. K_m has been determined to be 2.8 μ M for sulfide and 22 μ M for decylubiquinone (DUQ). The Cys160Ala and Cys356Ala variants have no activity. The activity assays conducted for the Cys128Ala variant showed 30–35% activity (\sim 70% activity loss) determined in the DUQ assay. However, in the FAD reduction assay, both the WT and the Cys128Ala variant have been found to be fully active (100%). This is the first observation that Cys128 is not involved in the FAD cofactor reduction step.

Structure determination

SQR from *At. ferrooxidans* was overexpressed in *Escherichia coli* and purified to homogeneity, as described elsewhere.²⁰ Crystals of the acceptor-bound SQR were grown from a solution containing protein and DUQ. The crystals of the native protein grew in space groups $P4_22_12$ and $P6_222$, whereas cocrystals of the complex with DUQ, as well as crystals of the Cys160Ala variant, grew only in space group $P6_222$. The native structure was solved in the tetragonal space group by molecular replacement using a C-terminally truncated molecule A of *Aq. aeolicus* SQR¹⁷ as search model; the SQR structure from *At. ferrooxidans* was refined to R_{work}/R_{free} of 16.7/20.0% (to 2.3 \AA resolution). The refined *At. ferrooxidans* SQR coordinates were used to obtain structural solutions for SQR in the hexagonal space group. The final values of R_{work} and R_{free} for each of these structures were 18.5/23.1% and 17.0/20.9% (to 2.05 \AA and 2.3 \AA resolutions), respectively, for the Cys160Ala variant and for the quinone-bound *At. ferrooxidans* SQR. The details of data collection and refinement are given in Table 1.

Structure of *At. ferrooxidans* SQR

The overall structure of *At. ferrooxidans* SQR is characteristic of the DSR family of proteins (Fig. 1). It comprises two tandem Rossmann fold domains and a very flexible C-terminal domain containing two amphipathic helices that are thought to provide for membrane binding^{17,21}; there also is one noncovalently bound FAD cofactor. The structures determined here are from two different crystal forms: tetragonal (PDB code 3kpi) and hexagonal (PDB code 3kpg). The hexagonal form was grown in the presence of a detergent, *n*-dodecyl β -D-maltoside (DDM), while the tetragonal form was grown in the absence of detergents. The SQR molecules determined in each crystal form are very similar, with an r.m.s.d. of 0.42 \AA between protein molecules for 412

Table 1. Data collection and refinement statistics

	SQR native (PDB code 3kpi)	SQR-DUQ (PDB code 3kpg)	SQR C160A (PDB code 3kpk)
<i>Data collection</i>			
Space group	$P4_22_12$	$P6_222$	$P6_222$
Cell dimensions			
a, b, c (Å)	131.7, 131.7, 208.9	150.8, 150.8, 82.0	150.1, 150.1, 81.7
α, β, γ (°)	90, 90, 90	90, 90, 120	90, 90, 120
Temperature (K)	100	100	100
Wavelength	0.97946	0.97950	0.97946
Resolution (Å)	50.0–2.30 (2.38–2.30)	20.0–2.30 (2.36–2.30)	50.0–2.05 (2.12–2.05)
R_{sym}	0.097 (0.986)	0.113 (0.987)	0.058 (0.814)
R_{rim}	0.104 (1.058)	0.116 (1.01)	0.063 (0.948)
R_{pim}	0.037 (0.384)	0.025 (0.218)	0.025 (0.566)
$I/\sigma I$	19.5 (1.94)	23.7 (4.08)	31.7 (1.55)
Completeness (%)	100 (100)	99.7 (100)	98.1 (85.5)
Redundancy	8.0 (7.6)	21.4 (21.5)	6.6 (3.8)
<i>Refinement</i>			
Resolution (Å)	40.7–2.3	19.91–2.3	34.6–2.1
Number of reflections	82,001	24,844	33,789
$R_{\text{work}}/R_{\text{free}}$	16.7/20.0	17.0/20.9	18.5/23.1
Number of atoms ^a	7371	3643	3596
Protein	6564	3209	3202
FAD	106	53	53
DDM	—	35	35
Sulfur	13	7	2
DUQ	—	23	—
Ions/other ^b	55/12	—	5
Water	621	316	299
B -factors (Å ²)			
Protein	56.5	46.6	50.4
FAD	43.2	30.5	31.6
DDM	—	42.7	46.5
Sulfur	67.7	58.6	72.0
DUQ	—	81.1	—
Ions	108.8	—	—
Water	60.8	50.3	50.5
Average	57.1	46.9	50.1
r.m.s.d.			
Bond lengths (Å)	0.014	0.004	0.007
Bond angles (°)	1.625	0.910	1.183

Values in parentheses are for the highest-resolution shell.

^a Number of nonhydrogen atoms present in the asymmetric unit.

^b "Ions/other" includes SO₄, 1,3-butanediol, or 1,2-propanediol.

C^α atom pairs. However, the last amphipathic helix in hexagonal form (residues 407–427) undergoes a major conformational change. Several residues of the N-terminus of this helix partially unwind; as a result, it becomes shorter and changes its orientation. The last amphipathic helix is very flexible even within the same crystal form. The structures solved from several hexagonal crystals showed that the last helix has slightly different conformations in each crystal (data not shown). Its B -factors are highly elevated. The last 7 residues (tetragonal form) and the last 16 residues (hexagonal form) have no electron density and have not been included in our structural models. It is likely that the flexible part of the SQR molecule keeps mobile in the membrane environment. Superposition of the two structures is shown in Fig. 1.

There are two SQR molecules in the asymmetric unit of the tetragonal crystal form (Fig. 2) and one molecule in the asymmetric unit of the hexagonal crystal form. The crystallographic dimer in the tetragonal asymmetric unit is formed largely by interactions between hydrophobic C-terminal

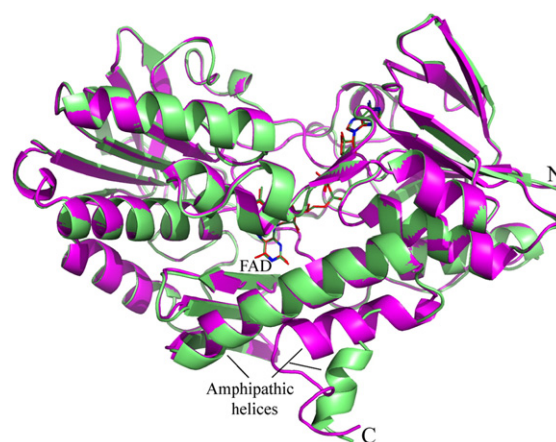


Fig. 1. Superposition of the structures of the tetragonal (magenta) and hexagonal (green) crystal forms of *At. ferrooxidans* SQR. The major conformational differences are observed in the C-terminal region; a few N-terminal residues of the last amphipathic helix of the hexagonal form of SQR partially unwind, and the helix changes its orientation.

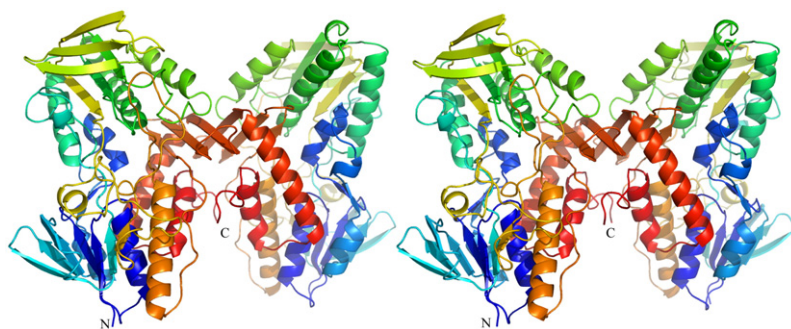


Fig. 2. The crystallographic dimer of *At. ferrooxidans* SQR in the tetragonal crystal form. Each protomer is represented in rainbow color: blue at the N-terminus, passing on to red at the C-terminus. The majority of contacts across the dimer interface occur between the putative membrane-interacting segments of the enzyme. As a result, this dimer cannot exist in the membrane.

regions that include the amphipathic helices of each protomer (Fig. 2). Similar dimers interacting via their C-terminal domains have also been observed in the hexagonal crystal form of this protein and in both *Aq. aeolicus* and *Acidia. ambivalens* SQR structures. It is very likely that all SQRs dimerize in solution via the largely hydrophobic membrane-interacting surfaces of the molecules. Most probably, these particular dimers are usually found by conventional methods. For *At. ferrooxidans* SQR, the asymmetric unit dimer has a solvent-inaccessible interface of 1154 \AA^2 per protomer. The solvation free energy of this interface is -14.8 kcal/mol , indicating the predominantly hydrophobic nature of dimer interactions. It has a positive ΔG_{diss} (4.2 kcal/mol) upon its dissociation, confirming the stability of this dimer. Calculations of the dissociation constant $K_{\text{diss}} = \exp(-\Delta G_{\text{diss}}/RT)$ give $K_{\text{diss}} = 10^{-3} \text{ M}$, which means that the dimer concentration will be less than 10% at physiological protein concentrations (below $0.1 \text{ mM} = 5 \text{ mg/ml}$); at a protein concentration below 0.01 mM , the dimer concentration will be less than 1%. In other words, the equilibrium shifts sharply towards monomers at lower protein concentrations, as has been confirmed by size-exclusion chromatog-

raphy (data are not shown). However, these dimers should dissociate for membrane insertion. The thermodynamic analysis of possible assemblies using the European Molecular Biology Laboratory–European Bioinformatics Institute Protein Interfaces, Surfaces, and Assemblies server does not find any other stable multimers in solution. The only dimer that would exist in solution at moderate and higher protein concentrations should be the dimer discussed above. However, in the membrane environment, the entropy term ΔS_{diss} should only slightly change for the membrane-bound multimer upon its dissociation, and it can be disregarded. Now, the binding energy ΔH will determine the stability of assemblies. The possible multimer should also allow the proper positioning of the amphipathic helices in the membrane.

Based on this requirement and the examination of all the interfaces, a probable biological dimer (with a common interface in two crystal forms) is suggested (Fig. 3). It is different from the trimer that has been proposed for *Aq. aeolicus* SQR.¹⁷ This difference in the oligomeric state of the SQR enzyme in the membrane is unlikely to be important from a mechanistic point of view. The superposition of

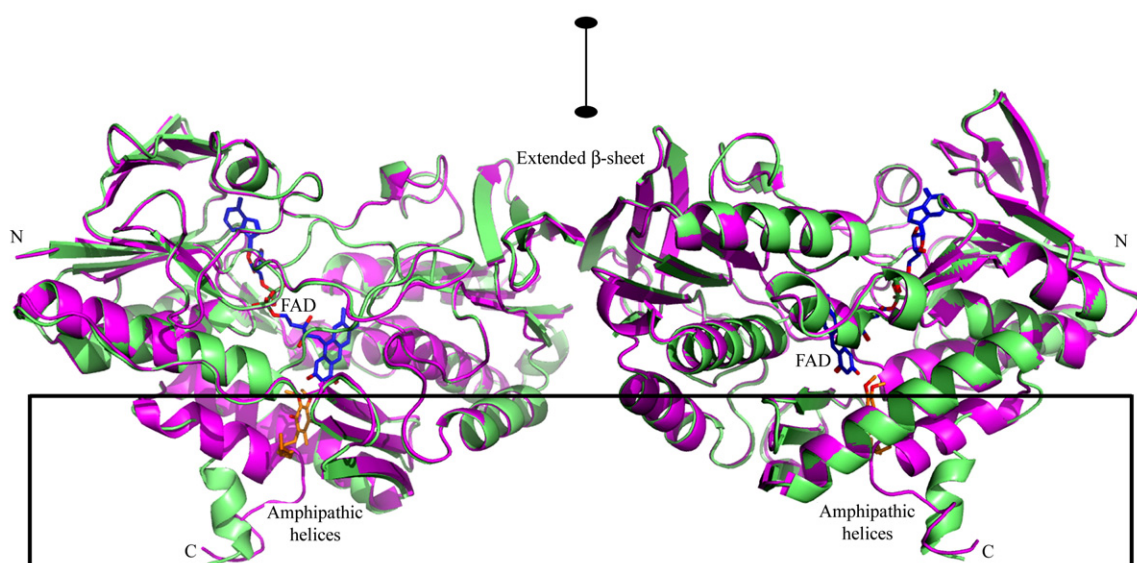


Fig. 3. The biological dimer present in both crystal forms: tetragonal (magenta) and hexagonal (green). The two protomers are related by a crystallographic 2-fold axis. Two β -sheets, one from each protomer, align in an extended β -sheet on top of the dimer. DUQ (in orange below the FAD cofactor) delimits the upper surface of the membrane. The two amphipathic helices penetrate into the membrane (rectangle) by about 20 \AA (height of the rectangle).

the biological dimer structures of the two crystal forms (tetragonal and hexagonal) is shown in Fig. 3. The dimer interface buries approximately 620 Å² (per protomer) of solvent-accessible surface area. It is formed mostly by the β 17-strands of an extended anti-parallel β -sheet (residues 247–254) from each protomer, which are related by a crystallographic 2-fold axis. Each protomer has an elliptical shape with approximate dimensions 45 Å × 67 Å; the longer elliptical axis is almost doubled in the dimer (54 Å × 126 Å). This arrangement of the protomers in the dimer puts the C-terminal domains with the amphipathic helices on one side of the dimer below the equatorial plane of the ellipsoid so that they could penetrate into the membrane, whereas the extended β -sheet is situated on the opposite side away from the membrane surface. The amphipathic helices make a sharp angle ($\sim 30^\circ$) with the equatorial plane that is perpendicular to the crystallographic 2-fold axis, but they are very flexible and could easily become parallel with the membrane surface. The most flexible C-terminal segment that protrudes from the protein bends sharply in the direction of the presumptive membrane. The depth of the insertion could be estimated using the supposition that both molecules of the biological dimer are equally inserted and that both benzoquinone rings of the substrate determine the top level of the phospholipid bilayer. It has been estimated to be about 20 Å (Fig. 3), which is approximately one-half of the membrane thickness.²² A similar membrane-bound biological dimer would likely form in *Acidithiobacillus ambivalens* SQR, in which dimerization might occur via the β -strands (residues 51–61) and the amphipathic helices would be equally inserted in the membrane. In *Aquaspirillum aeolicum* SQR, a dimer-of-trimers organization has been found¹⁷ in the asymmetric unit. It allows for the amphipathic helices to be in a hydrophobic environment that mimics the membrane. The amphipathic helices, as well as the whole trimers, are almost parallel with the equatorial plane and, consequently, to the presumable membrane surface. It was suggested that they penetrate the membrane to a depth of approximately 12 Å.¹⁷

SQR multimers (dimers or trimers) do not affect the catalytic mechanism. Their possible role could be to provide stability to the protein orientation in the membrane. A change in the orientation could put the FAD cofactor and the electron acceptor (ubiquinone or menaquinone) floating in the membrane in unfavorable positions.

The *At. ferrooxidans* SQR structure exhibits an overall fold that is quite similar to those of the other reported homologues. The superposition of the *At. ferrooxidans* SQR structure with the structures of *Aq. aeolicum* SQR (PDB codes 3hyw, 3hyv, and 3hyx; Fig. 4), *Acidithiobacillus ambivalens* SQR (PDB code 3h8l), and FCC from *Al. vinosum* (PDB code 1fcd) shows that the present structure is more closely related to the *Aq. aeolicum* SQR structure than to the two latter structures, with r.m.s.d. values of about 1.3 Å, 2.75 Å, and 2.26 Å for 401, 370, and 348 C α atoms, respectively. The largest differences occur in the C-terminal domains containing the amphipathic helices.

Redox active site and bound ligands

The active site of *At. ferrooxidans* SQR includes two cysteines (Cys160 and Cys356), the FAD cofactor, and, possibly, a third cysteine residue (Cys128) (Fig. 5). The FAD cofactor plays a central role in the catalytic mechanism. It accepts electrons from a sulfide species and transfers them to acceptor molecules (ubiquinone or menaquinone). The cofactor position in the *At. ferrooxidans* SQR structure is similar to that in other DSR proteins; it is bound in the first Rossmann fold domain. It makes a network of van der Waals contacts with the protein; 11 of these contacts are hydrogen-bonding and electrostatic interactions. The most important interactions involve the isoalloxazine ring (atoms O4 and O2), oxygen atoms of the phosphate groups (atoms O1P, O2P, and O2A), the ribose moiety (atom O3B), and the adenine moiety (atoms N1A and N6A) of the FAD. They form hydrogen bonds with the main-chain nitrogen atoms of Thr11, Gly12, Ala78, Ile302, Gly322, and Phe357; with the main-chain oxygen atom of Ala78; and with the side-chain nitrogen and

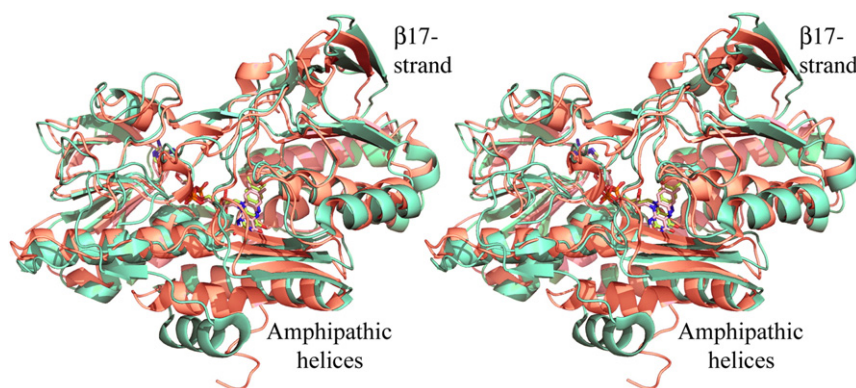


Fig. 4. Superposition of the *At. ferrooxidans* SQR structure (salmon) with the *Aq. aeolicum* SQR structure (green). FAD cofactors are represented by sticks. The major difference between the two structures occurs in the C-terminal domains containing amphipathic helices. The β 17-strand forms a dimer interface in *At. ferrooxidans* SQR.

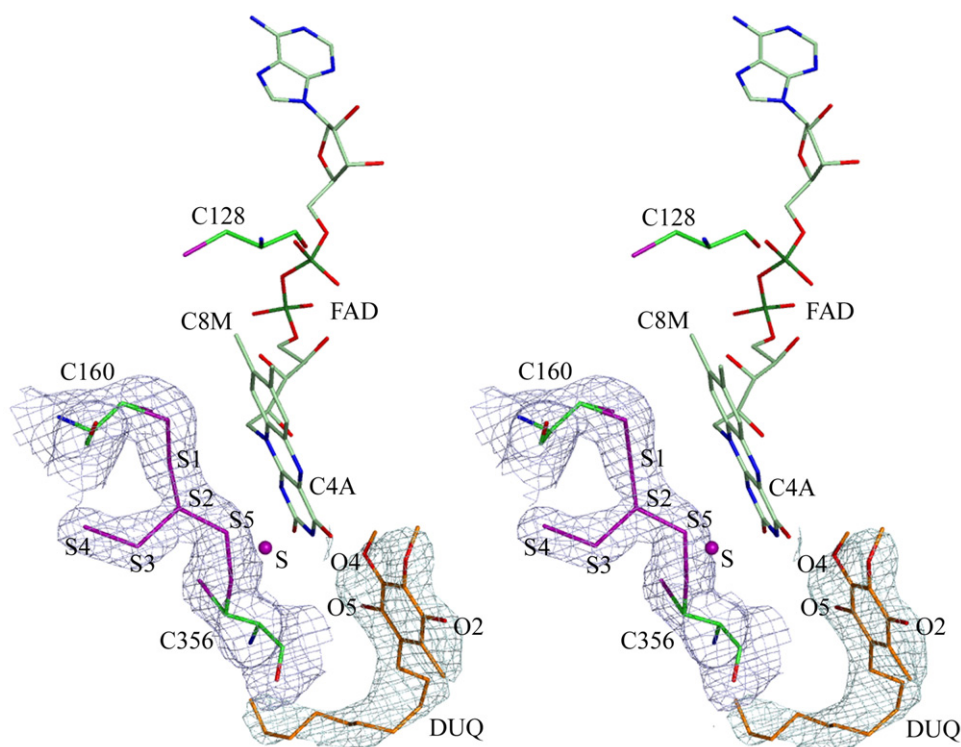


Fig. 5. The redox active site and the ligands in the SQR–DUQ complex. Two active-site cysteines (Cys160 and Cys356; green carbon atoms) lie on the *re* side of the isoalloxazine ring of FAD (lime carbon atoms); DUQ (orange sticks) is located on the *si* face of the isoalloxazine ring of FAD. Cys128 (green carbon atoms) is not modified. Sulfur atoms (magenta) form a branched pentasulfane that is covalently bound to both cysteines. The S⁵ atom covalently attached to Cys356 is close to the C4A atom of FAD (distance is less than 3.5 Å). A putative sulfur atom (S) is at a hydrogen-bonding distance from Cys356 and Glu166 (data not shown). The latter is thought to be the general base for abstracting protons from hydrogen sulfide. The $2|F_o| - |F_c|_{\alpha_c}$ electron density omit map is contoured at the 0.8σ level in the region of DUQ, Cys160, and Cys356.

oxygen atoms of Lys391 and Ser34. The O1P atom of the phosphate group is also involved in capping interaction with the N-terminus of the α 1 helix (Gly12); this interaction is due to the dipole moment of the helix that is positively charged at the N-terminus. It makes an electrostatic interaction with the negatively charged phosphate group. As a result of multiple interactions with the enzyme, the average *B*-factor of the FAD molecule is very low; in fact, it is lower than the average *B*-factor for the protein molecule (Table 1). Interestingly, the second Rossmann fold domain does not bind a second nucleotide (as was discussed previously),¹⁸ in contrast to some of the related oxidoreductases (for instance, the lipoamide dehydrogenase; PDB code 1lv1). The latter binds FAD and NAD cofactors simultaneously. However, in SQR, the binding of the second nucleotide is prevented by the loop (residues 155–160) that occupies the space where the second nucleotide would bind. This loop contains one of the active-site cysteine residues, Cys160.

The mode of FAD binding in *At. ferrooxidans* is different from those in other DSR proteins. The three most closely related structures contain a covalently bound FAD cofactor (via its C8M atom) that connects to the Cys128 (hereafter in *At. ferrooxidans* numbering, unless specifically mentioned) sulfur atom directly^{18,19} or through a disulfide bridge.¹⁷ In *At. ferrooxidans* SQR, the cofactor has no covalent

bond to Cys128, even though the Cys128 S^γ atom is 3.86 Å from C8M. This fact was also confirmed in another experiment in which FAD was removed from the trichloroacetic-acid-treated protein by dialysis (data not shown).

The cofactor is situated in the vicinity of the two active-site cysteines Cys160 and Cys356. The distance between the C4A atom of the isoalloxazine ring of the FAD cofactor and the S^γ atoms of Cys160 or Cys356 is ~ 5 Å. These two cysteine residues are positioned on a line that is almost parallel with the plane of the isoalloxazine ring, on its *re* side (Fig. 5). The electron density of the thiol groups of Cys160 and Cys356 extends in both crystal forms to form adducts with additional sulfur atoms. Cys356 has been modeled as a disulfide that is covalently connected to a tetrasulfide at Cys160 (in hexagonal form) or to a trisulfide (in tetragonal form). The resulting arrangement of sulfur atoms can also be considered as a branched pentasulfide or tetrasulfide molecule covalently attached to both cysteines (Figs. 5, 9, and 10). The occupancy of the sulfur atoms in the tetragonal form refined to an average of 0.58, whereas the occupancy varied from 0.5 to 1.0 in the hexagonal form, with the S5 atom having the highest occupancy.

A species (tentatively determined as sulfide, based on an occupancy of 1.0, to fit the spherical $|F_o| - |F_c|$ electron density peak at 15.8σ) was found

bound in the pocket close to Cys128 in the tetragonal crystal form and in some hexagonal crystals. It makes a network of hydrogen bonds with the N^δ atom of His132, the O^γ atom of Ser126, and the backbone N atoms of Thr129 and Cys128. However, it does not make a covalent bond with Cys128; it is situated at a distance of 4 Å from the S^γ atom of Cys128. It may form a Cys128 disulfide at some point in the catalytic cycle. The role of Cys128 and its possible disulfide is discussed more fully in Discussion.

Additional electron density peaks that have probably originated from the expression and purification in *E. coli* were present in all structures. Based on the shape of the electron density, several of them have been modeled as glycols (1,3-butanediol or 1,2-propanediol). Several flat oval blobs were stacked against aromatic rings of tryptophan and tyrosine residues (Trp52, Tyr195, Tyr223, and Tyr383) on the molecular surface, indicating an affinity for aromatic rings and possible additional sites for ubiquinone binding. Several potential sulfate-binding sites have been identified in the tetragonal crystal form. No sulfate ions have been detected in hexagonal form. DUQ binding is discussed more fully below.

Cys160Ala variant

Crystals of the Cys160Ala variant are isomorphous with those cocrystallized with DUQ. The structure of the Cys160Ala variant (PDB code 3kpk) is very similar to those of the native protein. Superposition of the variant structure with the structures of the native protein in complex with DUQ or with the native protein in the tetragonal crystal form gives r.m.s.d. values of approximately 0.28 Å for 418 C^α atom pairs and 0.49 Å for 412 C^α atom pairs. The distance between C^β atoms of Ala160 and Cys356 (9.2 Å) in the variant structure is slightly larger than the average equivalent distance for the Cys160 and Cys356 residues in the native protein structures (8.8 Å). There are no additional electron density peaks other than that for the methyl

group in the vicinity of the Ala160 C^α atom. However, some positive electron density appeared in close proximity to the S^γ atom of Cys356, and it was modeled as a disulfide at Cys356. The sulfur atom of the disulfide was refined to an occupancy of 1.0 at the S–S covalent bond distance (2.08 Å) from the S^γ atom of Cys356 in alternative conformations. The density indicates that the sulfide substrate can interact with Cys356 directly in the absence of the redox active disulfide bridge, but the reaction stops there. Three water molecules are located within hydrogen-bonding distance of the Cys356 disulfide. No polysulfide chains were detected, and there was no catalytic activity associated with the Cys160Ala variant.

Complex with DUQ

Soaking pregrown hexagonal native crystals with DUQ did not result in quinone binding. The soaked and unsoaked crystals revealed an electron density peak close to the isoalloxazine ring of FAD that was not consistent with the DUQ structure (data not shown). The quinone-binding site has been determined from the structure of SQR that was cocrystallized with DUQ. The cocrystals belonged to the hexagonal crystal form space group $P6_22$ and were isomorphous with the hexagonal unbound native protein (not reported here) and the Cys160Ala variant crystals (Table 1). DUQ has an atomic occupancy factor of 1.0 in the binding site. The quinone position is slightly different from that in the *Aq. aeolicus* SQR–quinone structure. The majority of the contacts of DUQ atoms with the protein atoms are hydrophobic. The aromatic ring of the quinone moiety is situated between the two benzene rings of Phe394 and Phe357 (Fig. 6). Out of a total of 18 contacts at a distance of 3.6 Å, 10 contacts to these two phenylalanine residues are made. The other contacting residues are Phe41, Pro43, Gly322, Tyr323, Asn353, and Tyr411. The benzoquinone head is also close to the isoalloxazine ring; the

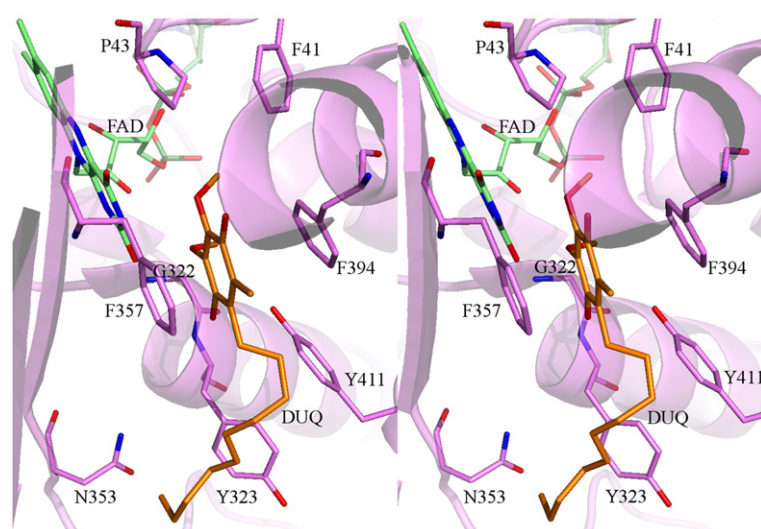


Fig. 6. The aromatic ring of DUQ (orange sticks) is sandwiched between two benzene rings of Phe357 and Phe394 (magenta). The majority of the interactions with the enzyme are hydrophobic.

distance between the O4 atom of the quinone and the O2 atom of FAD is less than 3 Å (Fig. 5). The hydrophobic decyl chain points backwards from the amphipathic helices. It makes very few contacts with the protein (residues Tyr323, Asn353, and Tyr411). Superposition of the cocrystallized SQR–DUQ complex structure with the native tetragonal form crystal structure showed that the side chain of Met418, a residue situated at the C-terminus of the second amphipathic helix, would occupy the benzoquinone position, whereas Leu415 would have very close contacts (1.7–2.1 Å) with the quinone tail. This observation indicates that the second amphipathic helix of the tetragonal form would have to rearrange to allow quinone binding.

Electrostatic surface and channels

Electrostatic surface analysis shows that the molecule of SQR is divided into positively and negatively charged regions that are situated on opposite sides of the molecule (Fig. 7a and b). The positively charged region of the SQR molecule (Fig. 7b) mostly contains both amphipathic helices and other segments of the protein that potentially interact with the negatively charged region of the phospholipid bilayer. The membrane-binding part contains a large number of Arg, Lys, and His residues and is rich in hydrophobic residues that

are necessary to maintain the protein inside the hydrocarbon layer of the membrane.

The electrostatic surface representation also reveals several channels that connect the interior of the molecule to the outside neighboring environment. The largest of these channels contains the FAD cofactor; its isoalloxazine ring is located deep in the interior of SQR (Fig. 7a). This channel is much wider than is required to accommodate FAD, so the rest of the channel is filled with a series of ordered solvent molecules. Cys128 is close to this channel, but its sulfhydryl group is turned away from it. The sulfide species bound in the pocket close to Cys128 has no direct access to the channels, but it is separated from the bulk solvent by only the imidazole ring of Hys132. Both active-site cysteine residues Cys160 and Cys356, as well as the important proton acceptor Glu166, have access to a smaller sulfide channel. Cys160 is more solvent accessible than Cys356, as the former is situated at the wider part of the sulfide channel, and the latter has access to the narrower part of the channel. The sulfide channel in *At. ferrooxidans* SQR is slightly different from those in *Acidithiobacillus ambivalens* and *Aquaspirillum aerophilum*. DUQ and dodecyl maltoside (DDM, the detergent) are located in two other channels. One of these channels occupied by DDM in the hexagonal crystal form is hydrophobic; it would open into the internal part of the membrane and

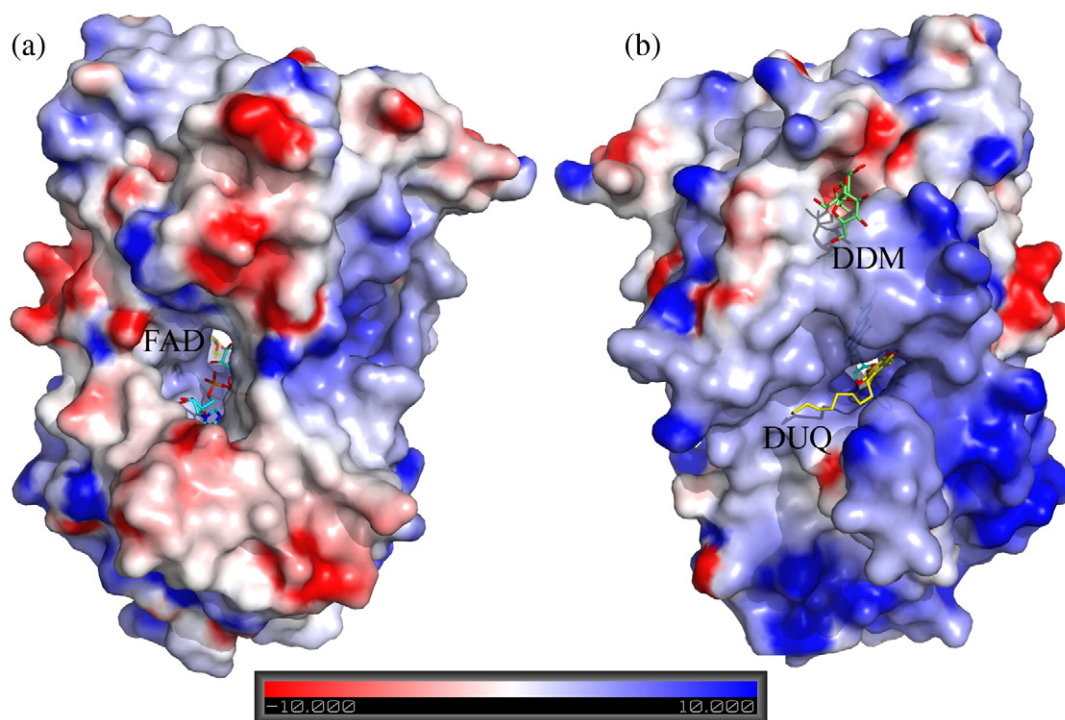


Fig. 7. The electrostatic surface of SQR and channels through the molecule calculated by the program GRASP. (a) One side of the SQR molecule has a largely negative (red) surface. The adenine moiety of the FAD cofactor is seen (cyan sticks) in the opening of the largest channel. (b) The opposite side of the molecule has a largely positive (blue) surface. DUQ (yellow sticks) and DDM (the detergent; green sticks) are located in smaller channels that are connected to the large channel occupied by FAD.

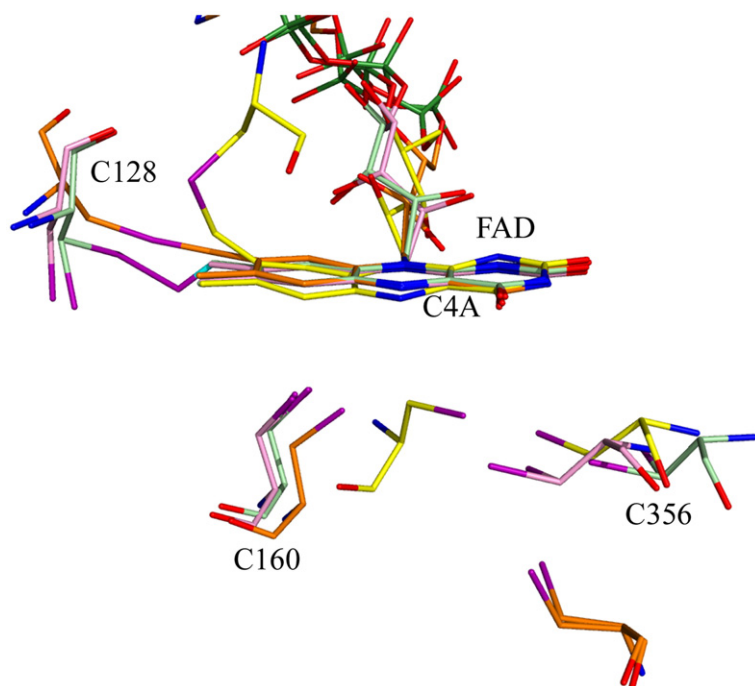


Fig. 8. Superposition of the active sites of four analogous sulfide-oxidizing enzyme structures. Only the atoms of the FAD cofactors were used for the superposition. The distance between the C $^{\alpha}$ atoms of Cys160 and the C $^{\alpha}$ atoms of Cys356 in *At. ferrooxidans* SQR (pink) is 2 Å shorter than that in *Aq. aeolicus* SQR (pale green) and is similar to the equivalent distance in *Acidia. ambivalens* SQR (orange). The equivalent residues in *Al. vinosum* FCC (yellow) are present as a disulfide bridge. The FAD cofactor is covalently attached to Cys128 in homologous SQRs from *Acidia. ambivalens* and *Aq. aeolicus*, as it is to the equivalent cysteine in FCC (Cys42 in FCC numbering). It is thought that Cys42 of FCC is not involved in the catalytic mechanism. The polysulfide bridges between Cys160 and Cys356 are not shown (sulfur atoms in magenta).

could possibly serve as a product release pathway, as proposed for a similar hydrophobic channel in *Aq. aeolicus* SQR.¹⁷ The hydrophobic tail of DDM points into the interior of the protein molecule and comes very close to Cys356 and the polysulfur

product. The distance between the C $^{\alpha}$ atom of Cys356 and the C12 atom of DDM is less than 4 Å. The hydrophilic head of DDM sticks out of the channel, exposed to the bulk solvent (Fig. 7b). DUQ is oriented in a different way; its polar head is

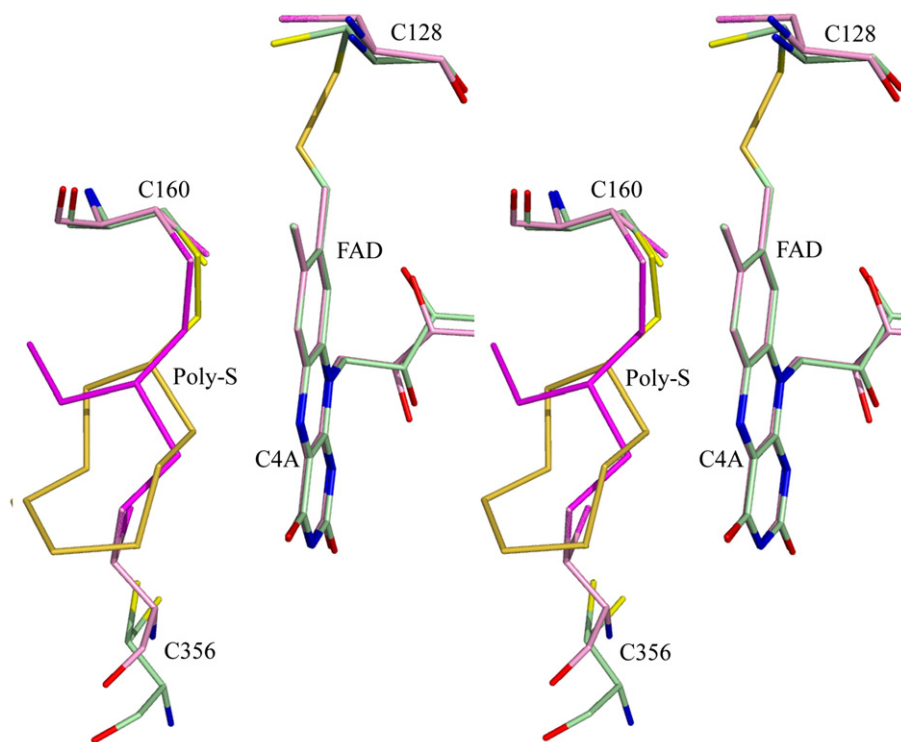


Fig. 9. A detailed comparison of the active sites of *At. ferrooxidans* SQR (pale pink; sulfur atoms in magenta) and *Aq. aeolicus* SQR (lime; sulfur atoms in yellow). Only the atoms of the FAD cofactors were used for this superposition. The positions of Cys128 and Cys160 are very similar, whereas Cys356 is slightly moved away by 2 Å from the Cys160 in *Aq. aeolicus* SQR. Cys160 and Cys356 are connected by a branched polysulfide bridge in *At. ferrooxidans*. These cysteines are not bridged in *Aq. aeolicus*.

inserted deep into the protein interior, whereas its hydrophobic tail points to the outside of the molecule. This is the region of the enzyme that is proposed to be inserted into the membrane.

Discussion

The molecular mechanism of the electron transfer reaction catalyzed by SQR is not fully understood

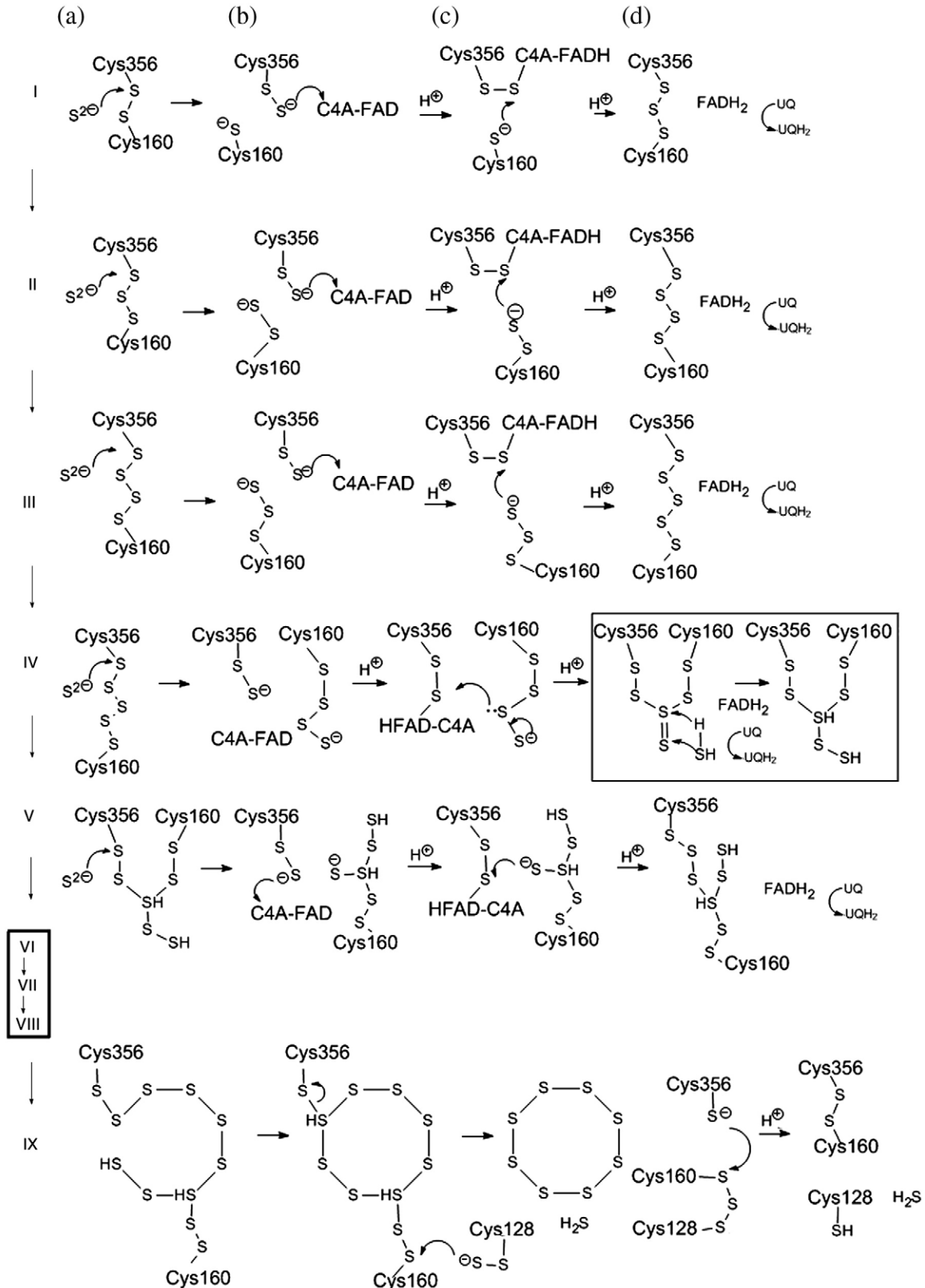


Fig. 10 (legend on next page)

due to the complexity of the mechanism and the scarcity of structural information. Three cysteine residues (Cys160, Cys356, and Cys128) have been shown to be necessary components of the enzymatic reaction. Substitution of any of the two residues (Cys160 or Cys356) leads to a complete loss of activity; substitution of the third residue Cys128 causes a substantial loss (~70%) of activity. Several hypotheses concerning the catalytic mechanism of electron transfer by SQRs have been suggested. The conventional mechanism includes the formation of a Cys160 thiolate^{6,18} or a Cys160-S-S⁻ disulfide¹⁷ that attacks the C4A atom of FAD. The polysulfide chain grows on Cys356. The role of the third cysteine of the active site (Cys128) is to maintain a redox active disulfide bridge with Cys160 and/or to maintain the position of the flavin ring of FAD.^{6,17,18} An alternative mechanism was suggested for *Aq. aeolicus* SQR; this mechanism involves the formation of a Cys128-S-S⁻ disulfide species that attacks the C8M atom of FAD. Electron transfer occurs during this step.¹⁷ This leads to the formation of a transient Cys128-S-S⁺ cation. The trisulfide bridge Cys128-S-S-Cys160 forms after the recombination of the above cation with the Cys160 thiolate. The role of Cys356 is to take over the growing polysulfide chain and, as a result, to recover the Cys160 thiolate. However, this mechanism is not applicable to FCC.

At. ferrooxidans SQR shares many structural and biological properties with other SQRs and with FCC, particularly with *Aq. aeolicus* SQR. The relative spatial positions of the three essential cysteines are similar to a certain degree in all four homologues (Figs. 8 and 9). The largest structural difference is found in FCC. The cysteine residue equivalent to Cys128 in FCC is Cys42; it is covalently attached to FAD and is situated on the other side of the isoalloxazine ring. Cys42 of FCC does not directly participate in sulfur polymerization. In SQR from *At. ferrooxidans*, Cys128 and Cys160 are situated on loop segments that are separated from the N-termini of corresponding helices by one (for Cys160) or two (for Cys128) residues; Cys356 is located in the middle of a β -strand. The initial redox active disulfide bridge may be located between Cys160 and Cys356 similarly to FCC, where the one equivalent to the Cys160-S-S-Cys356 disulfide bridge was actually observed.

Although the previously suggested conventional mechanisms^{17,18} might be applicable in the case of *At. ferrooxidans* SQR (with the Cys160 thiol/disulfide being the nucleophile), we propose an alternative mechanism that involves Cys356-S-S⁻ as the nucleophile that most probably attacks the C4A atom of FAD. The details of this mechanism are presented in Fig. 10. The initial nucleophilic attack of S²⁻ on the Cys160-Cys356 disulfide bridge leads to a thiol at Cys160 and to a disulfide at Cys356 (Fig. 10, Ia and b); the latter attacks the C4A atom of the isoalloxazine moiety. The Cys356-S-S-C4A adduct is formed, and one electron is transferred to the isoalloxazine ring (Fig. 10, Ic). The Cys160-S⁻ thiol then attacks the Cys356-S-S-C4A-FAD adduct, releasing the FAD cofactor and forming a trisulfide bridge between Cys160 and Cys356 (Cys356-S-S-S-Cys160; Fig. 10, Ic and d); in this step, a second electron is transferred to the isoalloxazine ring that is now fully reduced. Protons that are added to the reduced cofactor likely come from solvent. Repetition of the abovedescribed steps leads to elongation of the polysulfide chain that grows on Cys160 (Fig. 10, II-VIII). The elongation reaction stops when stereochemical constraints prevent further incorporation of sulfur atoms. The octasulfur ring is released from Cys160 as depicted (Fig. 10, IX). The role of Cys128 (most likely in the form of a disulfide) is confined to the release of the polysulfur product. The sulfide species observed in the pocket near Cys128 could produce the Cys128 disulfide that can reach the S ^{γ} atom of Cys160. The release of the hydrophobic polysulfur product could likely occur as proposed¹⁷ through the hydrophobic channel occupied by DDM in the present structures, or less likely through the sulfide channel that connects Cys160 with the exterior of the molecule. The other side of the sulfide channel going to Cys356 is much narrower, and only water and sulfide ions can move through it.

The unique point of this hypothesis is that the S⁻ atom of the Cys356-S-S⁻ disulfide is the nucleophile that attacks C4A at the start of each cycle. This hypothesis is supported by the fact that the distance of the S⁻ atom of the Cys356 disulfide to the C4A atom of flavin is around 3.2–3.5 Å, whereas the distances between the other potential nucleophilic sulfur atoms of Cys160 thiol or the Cys160-S-S⁻ disulfide and the C4A atom of flavin are too long for

Fig. 10. The proposed mechanism of sulfide oxidation: a sulfide ion attacks S ^{γ} of Cys356 in each elongation cycle (I–VIII), resulting in the transfer of two electrons to FAD and the attachment of a sulfur atom to the polysulfide bridge. Cycle I: A sulfide ion attack on Cys356-S ^{γ} breaks the disulfide bridge, consequently producing a disulfide on Cys356 and a thiol on Cys160. Cys356 disulfide attacks the C4A atom of FAD, forming a covalent adduct with C4A-FAD, and one electron is transferred to the isoalloxazine ring. Cys160 thiol attacks the adduct and releases FAD. A second electron is transferred. FAD is now fully reduced and will transfer the electrons to the ubiquinone pool in the membrane. Cycles II–VIII repeat the steps of cycle I (details of cycles VI–VIII are not shown). The polysulfide chain grows on Cys160. The sulfur atom of the polysulfide chain nucleophilically attacks the covalent adduct of Cys356 disulfide with FAD. Formation of the branched polysulfide bridge may occur as shown in cycle IV. The boxed intermediate products are consistent with the structures determined here. Possible octasulfur ring formation and its separation from Cys160 involve a nucleophilic attack most like from Cys128 disulfide.

such a nucleophilic attack (Fig. 5). It makes Cys160 a less likely—although not impossible—candidate for the role of the nucleophile. The finding that the octasulfur ring in *Aq. aeolicus* SQR¹⁷ is attached to Cys160 also supports our proposed mechanism in which the polysulfide grows on Cys160. As the Cys128Ala variant retains full activity in the FAD reduction assay, it should be excluded as a potential nucleophile in the electron transfer to FAD. The fact that it is impaired in the DUQ assay indicates that the reaction stops when the polysulfur product accumulates on Cys160, and thus the reaction turnover is diminished.

The abstraction of protons from hydrogen sulfide molecules and the consequent addition of protons to the reduced cofactor presumably occur either from the active-site base (the highly conserved Glu166) or from the proximity of abundant water molecules.^{17,18} For the protonation of the reduced ubiquinone, two candidate residues could be proposed: Tyr411 and Lys391. Tyr411 is situated on the last mobile helix; its hydroxyl group is close to the benzoquinone ring, and it is at a hydrogen-bonding distance from a water molecule. Lys391 is positioned farther away, on the other side of the DUQ; the N⁵ atom of Lys391 is 4.6 Å distant from the closest atom of the benzoquinone head (and 2.7 Å distant from the O4 atom of FAD), close to several water molecules. Both Tyr411 and Lys391 could potentially transfer protons from water to DUQ. Glu326 and Lys391 have been suggested as possible proton donors for reduced ubiquinone in *Aq. aeolicus*.¹⁷ However, in the structures presented here, the carboxyl group of Glu326 is oriented differently, and it is unlikely to be the proton donor to ubiquinone.

The intermediate products observed in the structures here were modeled as a trithiosulfurous acid (four sulfur atoms, in tetragonal form) or a branched pentasulfane (five sulfur atoms, in hexagonal form) covalently attached to the S^γ atoms of Cys160 and Cys356, as schematically shown in Fig. 10 (boxed structures). The branching of the polysulfur moiety was also observed in *Aq. aeolicus* SQR, in which the octasulfur ring is covalently attached to Cys160 (Fig. 9).

The sulfur derivatives of *At. ferrooxidans* SQR expressed in *E. coli* have been formed in the absence of any added sulfide. The *E. coli* expression host has been shown to produce sulfides endogenously in reductive environments.²³

The superposition of the active sites from *At. ferrooxidans* and *Aq. aeolicus* SQRs is shown in Fig. 9. Evidently, they represent different moments in the catalytic cycle. The polysulfur product in the *At. ferrooxidans* SQR structure is smaller than that in the *Aq. aeolicus* SQR structure; consequently, Cys160-Cys356 distances are significantly different for these structures. It appears possible for Cys160 and Cys356 in *At. ferrooxidans* to move slightly from each other during stepwise polysulfide chain elongation. The alternative could be formation of smaller polysulfide chains that can rearrange into stable octasulfur rings outside the protein.

The difference among the several proposed mechanisms of electron transfer reaction from

sulfides to FAD lies in assigning the nucleophile that attacks the flavin moiety. According to the other proposed mechanisms, the thiol group of Cys160 nucleophilically attacks the C4A atom of flavin,^{6,17,18} or Cys128 indirectly attacks the C8M atom of flavin via a persulfate species.¹⁷ Definitely, more studies are needed to answer the remaining questions and uncertainties.

Materials and Methods

Crystallization and data collection

At. ferrooxidans SQR was expressed, purified, and crystallized in tetragonal form, as described elsewhere.²⁰ Small changes in crystallization conditions were used to grow crystals of the hexagonal crystal form. They were grown in hanging drops from 30% polyethylene glycol 600, 0.1 M 2-[bis(2-hydroxyethyl)amino]-2-(hydroxymethyl)propane-1,3-diol (pH 5.5 or pH 6.5), 0.1 M magnesium sulfate, and 0.05% DDM. Cocrystals with DUQ were produced from the mixture of 10 mg/ml protein and 2 mM DUQ under these same crystallization conditions. Crystals for data collection were flash cooled in liquid nitrogen. Data were collected on beamline 9-2 at the Stanford Synchrotron Radiation Laboratory and on beamline 08ID-1 at the Canadian Light Source (Saskatoon) using a temperature of 100 K and MAR 325 or MAR 225 detectors. Raw data were processed with HKL-2000 suite²⁴ and XDS/XSCALE.²⁵

Structure determination and analysis

Molecular replacements were performed with MOLREP²⁶ and Phaser.²⁷ Refinement of the coordinates and atomic temperature factors was carried out using the Phenix package and a maximum likelihood target.²⁸ Model rebuilding at various refinement stages was performed using Coot.²⁹ Protein stereochemistry was analyzed by PROCHECK.³⁰ The program PyMOL³¹ was used to calculate r.m.s.d. values between analogous structures and to make figures. Calculations of the buried surface area (Å²) and the thermodynamic parameters of the possible assemblies were carried out with the European Molecular Biology Laboratory-European Bioinformatics Institute Protein Interfaces, Surfaces, and Assemblies server.³²

Enzymatic activity assay

Reduction of DUQ

SQR activity was spectroscopically measured by the decrease in absorbance at 275 nm due to the reduction of DUQ, as described previously.³³ The reaction mixture contained 25 μg/ml (0.5 μM) protein in 50 mM 2-[bis(2-hydroxyethyl)amino]-2-(hydroxymethyl)propane-1,3-diol (pH 6.5), 20 mM glucose, 50 μM DUQ, 1 U/ml glucose oxidase, and 10 U/ml catalase. Anoxic conditions were established by flashing with N₂. The reaction was started by the addition of 100 μM freshly prepared Na₂S. One unit of activity was defined as the amount of enzyme that catalyzed the reduction of 1 μmol of DUQ per minute.³⁴ Absorption spectra during the enzymatic reaction were measured at 275 nm. The differential extinction coefficient determined by the measurement of the difference spectra of oxidized and reduced DUQs is 12.5 mM⁻¹ cm⁻¹.

Reduction of FAD

FAD reduction assay was conducted by measuring spectroscopically the decrease in absorbance at 375 nm and 450 nm due to the reduction of FAD. The reaction mixture contained 1 mg/ml protein in 50 mM Mops and 0.5 mM NaCl at pH 7.0. The mixture was titrated with sodium sulfide to concentrations from 0.12 μ M to 1.52 μ M. Absorbance was measured in the range from 300 nm to 600 nm.

Accession codes

The coordinates and structure factors have been deposited in the PDB under accession codes 3kpi, 3kpg, and 3kpk.

Acknowledgements

We are very thankful for help with data collection on beamline 9-2 at the Stanford Synchrotron Radiation Laboratory and particularly to Pawel Grochulski on beamline 08ID-1 (Canadian Macromolecular Crystallography Facility) at the Canadian Light Source (Saskatoon). Research in the laboratories of M.N.G.J. and J.H.W. was supported by the Canadian Institutes of Health Research (CIHR FRN-37770, CIHR MOP-15292, and MOP-121065). M.N.G.J. also had funding support from the Alberta Heritage Foundation for Medical Research.

References

- Shibata, H., Takahashi, M., Yamaguchi, I. & Kobayashi, S. (1999). Sulfide oxidation by gene expressions of sulfide-quinone oxidoreductase and ubiquinone-8 biosynthase in *Escherichia coli*. *J. Biosci. Bioeng.* **88**, 244–249.
- Brasseur, G., Levican, G., Bonnefoy, V., Holmes, D., Jedlicki, E. & Lemesle-Meunier, D. (2004). Apparent redundancy of electron transfer pathways via bc(1) complexes and terminal oxidases in the extremophilic chemolithoautotrophic *Acidithiobacillus ferrooxidans*. *Biochim. Biophys. Acta*, **1656**, 114–126.
- Shahak, Y. & Hauska, G. (2008). Sulfide oxidation from cyanobacteria to humans: sulfide-quinone oxidoreductase (SQR). In *Advances in Photosynthesis and Respiration* (Hell, R., Dahl, C., Knaff, D. & Leustek, T., eds), (Springer, Netherlands), 27, pp. 319–335.
- Theissen, U., Hoffmeister, M., Grieshaber, M. & Martin, W. (2003). Single eubacterial origin of eukaryotic sulfide:quinone oxidoreductase, a mitochondrial enzyme conserved from the early evolution of eukaryotes during anoxic and sulfidic times. *Mol. Biol. Evol.* **20**, 1564–1574.
- Griesbeck, C., Hauska, G. & Schütz, M. (2000). Biological sulfide oxidation: sulfide-quinone reductase (SQR), the primary reaction. In Pandalai SG (ed) *Recent Research Development in Microbiology*, 4, pp. 179–203. Research Signpost, Trivandrum, India.
- Griesbeck, C., Schütz, M., Schödl, T., Bathe, S., Nausch, L., Mederer, N. *et al.* (2002). Mechanism of sulfide-quinone reductase investigated using site directed mutagenesis and sulphur analysis. *Biochemistry*, **41**, 11552–11565.
- Pham, V. H., Yong, J.-J., Park, S.-J., Yoon, D.-N., Chung, W.-H. & Rhee, S.-K. (2008). Molecular analysis of the diversity of the sulfide:quinone reductase (sqr) gene in sediment environments. *Microbiology*, **154**, 3112–3121.
- Vande Weghe, J. G. & Ow, D. W. (1999). A fission yeast gene for mitochondrial sulfide oxidation. *J. Biol. Chem.* **274**, 13250–13257.
- Vande Weghe, J. G. & Ow, D. W. (2001). Accumulation of metal-binding peptides in fission yeast requires hmt2+. *Mol. Microbiol.* **42**, 29–36.
- Goubern, M., Andriamihaja, M., Nübel, T., Blachier, F. & Bouillaud, F. (2007). Sulfide, the first inorganic substrate for human cells. *FASEB J.* **21**, 1699–1706.
- Wang, R. (2002). Two's a company, three's a crowd: can H₂S be the third endogenous gasotransmitter? *FASEB J.* **16**, 1792–1798.
- Boehning, D. & Snyder, S. H. (2003). Novel neural modulators. *Annu. Rev. Neurosci.* **26**, 105–131.
- Kimura, H. (2002). Hydrogen sulfide as a neuromodulator. *Mol. Neurobiol.* **26**, 13–19.
- Grieshaber, M. K. & Voelkel, S. (1998). Animal adaptations for tolerance and exploitation of poisonous sulfide. *Annu. Rev. Physiol.* **60**, 33–53.
- Parrino, V., Kraus, D. W. & Doeller, J. E. (2000). ATP production from the oxidation of sulfide in gill mitochondria of the ribbed mussel *Geukensia demissa*. *J. Exp. Biol.* **203**, 2209–2218.
- Yong, R. & Searcy, D. G. (2001). Sulfide oxidation coupled to ATP synthesis in chicken liver mitochondria. *Comp. Biochem. Physiol. Part B Biochem. Mol. Biol.* **129**, 129–137.
- Marcia, M., Ermler, U., Peng, G. & Michel, H. (2009). The structure of *Aquifex aeolicus* sulfide:quinone oxidoreductase, a basis to understand sulfide detoxification and respiration. *Proc. Natl Acad. Sci. USA*, **106**, 9625–9630.
- Brito, J. A., Sousa, F. L., Stelter, M., Bandejas, T. M., Vonnrhein, C., Teixeira, M. *et al.* (2009). Structural and functional insights into sulfide:quinone oxidoreductase. *Biochemistry*, **48**, 5613–5622.
- Chen, Z. W., Koh, M., Van Driessche, G., Van Beeumen, J. J., Bartsch, R. G., Meyer, T. E. *et al.* (1994). The structure of flavocytochrome *c*:sulfide dehydrogenase from a purple phototrophic bacterium. *Science*, **266**, 430–432.
- Zhang, Y., Cherney, M. M., Solomonson, M., Liu, J., James, M. N. G. & Weiner, J. H. (2009). Preliminary X-ray crystallographic analysis of sulfide:quinone oxidoreductase from *Acidithiobacillus ferrooxidans*. *Acta Crystallogr. Sect. F*, **65**, 839–842.
- Johnson, J. E. & Cornell, R. B. (1999). Amphitropic proteins: regulation by reversible membrane interactions. *Mol. Membr. Biol.* **16**, 217–235.
- White, S. H. & Wimley, W. C. (1994). Peptides in lipid bilayers: structural and thermodynamic basis for partitioning and folding. *Curr. Opin. Struct. Biol.* **4**, 79–86.
- Flint, D. H. (1996). *Escherichia coli* contains a protein that is homologous in function and N-terminal sequence to the protein encoded by the *nifS* gene of *Azotobacter vinelandii* and that can participate in the synthesis of the Fe-S cluster of dihydroxy-acid dehydratase. *J. Biol. Chem.* **271**, 16068–16074.
- Otwinowski, Z. & Minor, W. (1997). Processing of X-ray diffraction data collected in oscillation mode. *Methods Enzymol.* **276**, 307–326.

25. Kabsch, W. (1993). Automatic processing of rotation diffraction data from crystals of initially unknown symmetry and cell constants. *J. Appl. Crystallogr.* **26**, 795–800.
26. Vagin, A. & Teplyakov, A. J. (1997). MOLREP: an automated program for molecular replacement. *J. Appl. Crystallogr.* **30**, 1022–1025.
27. McCoy, A. J., Grosse-Kunstleve, R. W., Adams, P. D., Winn, M. D., Storoni, L. C. & Read, R. J. (2007). Phaser crystallographic software. *J. Appl. Crystallogr.* **40**, 658–674.
28. Afonine, P. V., Grosse-Kunstleve, R. W. & Adams, P. D. (2005). The Phenix refinement framework. *CCP4 Newsl.* **42**; contribution 8.
29. Emsley, P. & Cowtan, K. (2004). Coot: model-building tools for molecular graphics. *Acta Crystallogr. Sect. D*, **60**, 2126–2132.
30. Laskowski, R. A., MacArthur, M. W., Moss, D. S. & Thornton, J. M. (1993). PROCHECK—a program to check the stereochemical quality of protein structures. *J. Appl. Crystallogr.* **26**, 283–291.
31. DeLano, W. L. (2002). *The PyMOL Molecular Graphics System*. DeLano Scientific, Palo Alto, CA, USA.
32. Krissinel, E. & Henrick, K. (2007). Inference of macromolecular assemblies from crystalline state. *J. Mol. Biol.* **372**, 774–797.
33. Morton, R. A. (1965). *Spectroscopy of quinones and related substances*. (Morton, R. A., ed.), Academic Press. Inc., London, UK.
34. Shahak, Y., Klughammer, C., Schreiber, U., Padan, E., Herrman, I. & Hauska, G. (1994). Sulfide–quinone and sulfide–cytochrome reduction in *Rhodobacter capsulatus*. *Photosynth. Res.* **39**, 175–181.